JOURNAL OF SOLID STATE CHEMISTRY **49**, 65–76 (1983)

The Stability of the Phases in the Ln_2O_3–FeO–Fe_2O_3 Systems Which Are Stable at Elevated Temperatures (*Ln:* Lanthanide Elements and Y)

NOBORU KIMIZUKA,* AKIJI YAMAMOTO, AND HARUO OHASHI

National Institute for Research in Inorganic Materials, 1-1, Namiki, Sakura-mura, Niihari-gun, Ibaraki-ken, 305 Japan

AND TADASHI SUGIHARA† AND TOSHIMORI SEKINE‡

Department of Chemistry, Faculty of Science, Tokyo Institute of Technology, Meguroku, Tokyo, 152 Japan

Received January 3, 1983; in revised form March 8, 1983

Thermochemical data on $LnFeO_3$, $Ln_3Fe_5O_{12}$, and $(LnFeO_3)_nFeO$ ($n = 1$ and 2) which are stable in the Ln_2O_3–FeO–Fe_2O_3 systems at elevated temperatures are reevaluated and interpreted on the basis of a simple point charge ionic model (*Ln:* lanthanide elements and Y). As the radius of the *Ln* ion in each compound decreases, the $LnFeO_3$ compound (distorted perovskite type) becomes less stable, the $Ln_3Fe_5O_{12}$ compound (garnet type) is the most stable for Ln = Tb, and the $(LnFeO_3)_nFeO$ compounds (layered structures) become more stable. The stability of each phase is strongly dependent upon the fitting of *Ln* ion in *A*-site position for the perovskite structure, in the dodecahedral site position for the garnet structure, and in the octahedral site positions for the layered structure compounds, respectively.

It is qualitatively useful to estimate the Madelung energies of a series of isostructural phases on the basis of a simple point charge ionic model, especially as a guide for understanding a series of new phase diagrams which describe the isostructural phases.

Introduction

Since the lanthanide orthoferrites *Ln* FeO_3 (*Ln:* lanthanide elements and Y, distorted perovskite structure), the lanthanide iron garnets $Ln_3Fe_5O_{12}$ (garnet structure), and the $(LnFeO_3)_nFeO$ ($n = 1, 2, 3 \ldots$) with layered structures have magnetically interesting properties, the crystal structures of each compound have been thoroughly investigated by many researchers. Geller and Wood (*1*), Geller (*2*), Coppens and Eibschütz (*3*), Marezio *et al.* (*4*), and Marezio and Dernier (*5*) reported the structures of the $LnFeO_3$ and concluded that they are distorted perovskites (orthorhombic, space group *Pbnm*) in which the average Fe–O bond lengths of the octahedron are nearly constant and the corner-linked octahedra are more tilted toward each other, as the *Ln* ion in the *A*-site position changes from La to Lu. Geller and Gilleo

---

* To whom all correspondence should be addressed.

† Present address: Central Research Laboratory, Mitsubishi Metal Corporation, Omiya, Saitama, 330 Japan.

‡ Present address: Dept. of Earth Science, Monash University, Clayton, Victoria, 3168 Australia.

0022-4596/83 $3.00

(*6*), Euler and Bruce (*7*), Weidenborner (*8*), and Dukhovskya *et al.* (*9*) refined the crystal structures of the garnets $Y_3Fe_5O_{12}$, $Gd_3Fe_5O_{12}$, $Ln_3Fe_5O_{12}$ (*Ln:* Lu, Yb, Y, Gd, and Sm), and $Ln_3Fe_5O_{12}$ (*Ln:* Eu and Tb), respectively, showing the dependence of oxygen position parameters on the lanthanide ion in the dodecahedral position. The cations *Ln* and Fe in the garnet are located in the special positions. The Fe–O bond lengths in the tetrahedra and the octahedra in the $Ln_3Fe_5O_{12}$ garnets (cubic, space group $Ia3d$) depend slightly upon the constituent *Ln* cation.

As to thermochemical studies of the $LnFeO_3$, Katsura *et al.* (*10a*) reported the relationship between the standard free energies of formation of $LnFeO_3$ (*Ln:* La–Dy) from Ln_2O_3, Fe, and O_2, and the Goldschmid's tolerance factor. As the tolerance factor deviates from unity, the stability decreases. Navrotsky (*11*) discussed the relationship between the standard enthalpy of formation of perovskites ABO_3 (*A:* Ba, Sr, Ca, and Mg, *B:* Ti, Ge, Zr, Sn, and Hf) from the binary oxides at 298 K and the absolute value of $(1 - t)$, where t is a tolerance factor. As t deviates from unity, the stability drops off remarkably. Recently, our research group systematically established the phase diagrams of the Ln_2O_3–FeO–Fe_2O_3 systems at elevated temperatures under controlled oxygen partial pressures (10*a–g*) and thermogravimetrically measured the standard free energy changes of $LnFeO_3$, $Ln_3Fe_5O_{12}$, and $(LnFeO_3)_nFeO$ ($n = 1$ and 2) with new layered structures. These compounds were synthesized according to the following chemical reactions:

$$Fe + \tfrac{1}{2}Ln_2O_3 + \tfrac{3}{4}O_2 = LnFeO_3$$

$$5Fe + \tfrac{3}{2}Ln_2O_3 + \tfrac{15}{4}O_2 = Ln_3Fe_5O_{12}$$

$$2Fe + \tfrac{1}{2}Ln_2O_3 + \tfrac{5}{4}O_2 = LnFe_2O_4$$

$$3Fe + Ln_2O_3 + 2O_2 = Ln_2Fe_3O_7.$$

Kato *et al.* (*12a, b*), Matsui *et al.* (*12c*), Kimizuka *et al.* (*12d*), and Malaman *et al.* (*12e, f*) analyzed the crystal structures of $YbFe_2O_4$, $Yb_2Fe_3O_7$, $Yb_3Fe_4O_{10}$, and $Yb_4Fe_5O_{13}$ and concluded that they are homologous compounds with layered structures ($YbFe_2O_4$: $R\bar{3}m$, $Yb_2Fe_3O_7$: $P6_3mmc$, $Yb_3Fe_4O_{10}$: $R\bar{3}m$, . . .). Geradin *et al.* (*13*) discussed the relationship between the stability of the $LnABO_4$ phases (*A:* trivalent cation, *B:* divalent cation) with layered structures, and its constituent cations. Studies on the physical properties such as magnetic, electrical transport phenomena, Mössbauer spectroscopies, and neutron diffraction analysis for the $(LnFeO_3)_nFeO$ compounds are in progress by Siratori's group (*14*). Kimizuka and Takayama established the phase diagrams of the Yb_2O_3–Fe_2O_3–*M*O systems and the Yb_2O_3–Ga_2O_3–*M*O systems in air at elevated temperatures and reported the existence of $LnAMO_4$ compounds with a layered structure (*A:* Fe, Ga, and Al, *M:* Zn, Co., Cu, Mn, and Mg) (*15*). The catalytic activities of the $LnFeO_3$ compounds have been characterized; their thermochemical stability under reduced atmosphere is considered to be important for practical applications to sensor systems or to catalytic functions (*16*). In the present paper, we reevaluate the published thermochemical data of the phases in the Ln_2O_3–FeO–Fe_2O_3 systems at elevated temperatures and discuss their thermochemical stabilities correlated with the size of the lanthanide element ion in each phase, based upon a simple point charge ionic model.

Results and Discussion

Reevaluations of the thermochemical data of the Ln_2O_3–FeO–Fe_2O_3 systems in a temperature range of 1000 and 1400°C were performed. The data at 1000 and 1100°C are mainly taken from two theses (*17a, b*).

TABLE I

GIBBS FREE ENERGY CHANGE OF THE CHEMICAL REACTION Fe + $\frac{1}{2}$ Ln_2O_3 + $\frac{3}{4}O_2$ = LnFeO$_3$ (ΔG°(kcal/mole) ± 0.30)

*Ln*FeO$_3$	100°C (a)	1100°C (a)	1150°C	1200°C	1224°C	1250°C	1275°C	1297°C	1347°C	1400°C
LaFeO$_3$	−74.36	−71.29		−68.91(c)		−67.48(c)		−66.11(c)		−63.39(c)
PrFeO$_3$	−72.35	−68.89		−66.07(a)						
NdFeO$_3$	−71.36	−68.51		−65.68(c)		−64.14(c)		−62.81(c)	−61.57(c)	
SmFeO$_3$	−70.38	−67.05		−64.10(e)		−62.64(c)		−61.29(c)		
EuFeO$_3$	−69.86	−66.34		−63.29(d)	−62.72(c)	−61.99(c)		−60.56(c)		
GdFeO$_3$	−69.51	−66.16		−63.14(c)	−62.43(c)	−61.69(c)		−60.15(c)		
TbFeO$_3$	−68.59	−65.12	−63.05(a)	−61.78(a)	−61.47(c)	−60.69(c)	−59.56(c)			
DyFeO$_3$	−67.98	−64.32	−62.36(a)	−61.20(a)	−60.80(c)	−59.89(c)	−58.67(c)			
HoFeO$_3$	−67.54	−63.70	−61.63(b)	−60.46(b)		−59.23(b)				
ErFeO$_3$	−67.10	−62.99		−59.70(e)						
TmFeO$_3$	−66.23	−62.06	−59.74(b)	−58.72(b)		−57.41(b)				
YbFeO$_3$		−61.40		−58.17(f)						
LuFeO$_3$		−60.65	−58.36(b)	−57.52(b)		−56.09(b)				
YFeO$_3$				−59.80(g)						

Note. Refs. (a) *17a*, (b) *17b*, (c) *10a*, (d) *10e*, (e) *10g*, (f) *10d*, (g) *10c*.

(*A*) *Stability of the LnFeO$_3$ compounds (Ln: La–Lu and Y)*

In Table I, the free energy changes accompanying the formations of the *Ln*FeO$_3$ phases are listed. Mizusaki *et al.* (*18*) reported decomposition atmospheres of oxygen of the LaFeO$_3$ phase (1000–1400°C) using the CO_2–CO system as reducing atmosphere in a process for measuring electric conductivity and Seebeck coefficient of LaFeO$_3$. The results estimated from one of their figures are ΔH°(kcal/mole) = − 119.4 ± 1.0, ΔS° (e.u.) = −32.7 ± 1.0. Nakamura *et al.* (*19*) measured the same parameters of *Ln*FeO$_3$ (*Ln:* La, Sm, and Dy) using the CO_2–H_2 system at 1000 and 1200°C. Their results are as follows: $\Delta G^\circ(1273\text{ K}) = -74.02 \pm 0.31$ (kcal/mole), $\Delta G^\circ(1473\text{ K}) = -68.91 \pm 0.31$ (kcal/mole). Piekarczyk *et al.* (*20*) measured the dissociation oxygen partial pressures and the Gibbs free energy changes of the formation of YFeO$_3$ phase by means of a solid state galvanic cell in a temperature range of 900–1250°C. Their results are $\Delta G^\circ(\text{kJ/mole}) = -421.3 + 114.8T \pm 0.7$ ($1173 \leqq T \leqq 1523$ (K)). At 1200°C, $\Delta G^\circ = -60.3 \pm 0.2$ (kcal/mole) is in good agreement with the present value (see Table I). Tretyacov *et al.* (*21*) also reported the emf of the *Ln*FeO$_3$ (*Ln:* La, Pr, and Eu) in a temperature range of 950–1200°C and of YFeO$_3$ in a temperature range of 900–1100°C by means of a solid state galvanic cell method. Their results are LaFeO$_3$: $\Delta G^\circ = -110 - (-28.5)T$, Dy FeO$_3$: $\Delta G^\circ = -115.5 - (-31.6)T$, EuFeO$_3$: $\Delta G^\circ = -108.3 - (-31.0)T$, and YFeO$_3$: $\Delta G^\circ = -102.0 - (-28.8)T$. All these data indicate that $-\Delta G^\circ$ decreases as the radius of the constituent *Ln* cation decreases. ΔH° and ΔS° were estimated from the dependence of the free energy change on temperature. They are listed in Table II. (The data for *Ln*FeO$_3$ (*Ln:* Tb, Dy, and Sm) which were already published in (*10a*) are reevaluated since the temperature range was expanded.) $-\Delta H^\circ$ decreases with the decrease of the ionic radius of the *Ln* cation in the compounds; however ΔS° is actually constant. Schmalzried and Navrotsky (*22*) estimated the entropy change accompanying the oxygen production in the decomposition of the oxide compounds. According to one of their conclusions, the entropy

TABLE II

ENTHALPY CHANGE AND ENTROPY CHANGE: $Fe + \frac{1}{2}Ln_2O_3 + \frac{3}{4}O_2 = LnFeO_3$

$LnFeO_3$	ΔH°(kcal/mole)	ΔS°(e.u.)
$LaFeO_3$	−109 ± 3.0	−27 ± 1.0
$PrFeO_3$	−110 ± 3.0	−30 ± 1.0
$NdFeO_3$	−109 ± 3.0	−29 ± 1.0
$SmFeO_3$	−109 ± 3.0	−30 ± 1.0
$EuFeO_3$	−109 ± 3.0	−31 ± 1.0
$GdFeO_3$	−109 ± 3.0	−31 ± 1.0
$TbFeO_3$	−108 ± 3.0	−31 ± 1.0
$DyFeO_3$	−107 ± 3.0	−31 ± 1.0
$HoFeO_3$	−107 ± 3.0	−32 ± 1.0
$ErFeO_3$	−107 ± 3.0	−32 ± 1.0
$TmFeO_3$	−105 ± 3.0	−31 ± 1.0
$YbFeO_3$	−104 ± 3.0	−31 ± 1.0
$LuFeO_3$	−103 ± 3.0	−31 ± 1.0
$YFeO_3$		

change for the series of the present chemical reactions should be $44n$ ($n = \frac{3}{4}$ for the present case) = 33 (e.u.), which seems to be in good agreement with our results.

Nakamura (*23*) calculated the Madelung energies of the ABO_3 compounds (perovskite type phase, A = La, Sm, and Dy; B = Mn and Fe) and the Ln_2O_3 compounds, and concluded that the dependence of $-\Delta H^\circ$ of formation of the perovskites formed from the Ln_2O_3 and the Fe_2O_3, on the Ln ion is mainly attributable to the difference of Madelung energies of $LnFeO_3$ and Ln_2O_3. Although Nakamura calculated the Madelung energies without using the results of the crystal structure analyses for each compound, he successfully showed a rather good consistency be-

TABLE III

MADELUNG ENERGIES OF Ln_2O_3, $LnFeO_3$, AND $Ln_3Fe_5O_{12}$ (eV)

Ln_2O_3	Form	Ref.	$U(Ln_2O_3)$/mole	$LnFeO_3$	Ref.	$U(LnFeO_3)$/mole	$Ln_3Fe_5O_{12}$	Ref.	$U(Ln_3Fe_5O_{12})$/mole
La_2O_3	A	a	−147.01	$LaFeO_3$	g	−163.76			
Pr_2O_3	A			$PrFeO_3$	h	−165.06			
Nd_2O_3	A	a	−150.84	$NdFeO_3$	h	−165.48			
Sm_2O_3	B	b	−153.03	$SmFeO_3$	h	−166.35	$Sm_3Fe_5O_{12}$	j	−677.16
Eu_2O_3	B	c	−153.94	$EuFeO_3$	h	−166.73	$Eu_3Fe_5O_{12}$	k	−677.91
Gd_2O_3	B			$GdFeO_3$	h	−166.99	$Gd_3Fe_5O_{12}$	l	−678.86
Gd_2O_3	C								
Tb_2O_3	B	d	−155.96	$TbFeO_3$	h	−167.61	$Tb_3Fe_5O_{12}$	k	−680.94
Tb_2O_3	C								
Dy_2O_3	C	f	−157.59	$DyFeO_3$	h	−167.97	$Dy_3Fe_5O_{12}$	j	−682.89
Ho_2O_3	C	f	−158.46	$HoFeO_3$	h	−168.44	$Ho_3Fe_5O_{12}$		
Er_2O_3	C	f	−159.15	$ErFeO_3$	h	−168.74	$Er_3Fe_5O_{12}$		
Tm_2O_3	C	f	−159.89	$TmFeO_3$	h	−169.01	$Tm_3Fe_5O_{12}$		
Yb_2O_3	C	f	−160.89	$YbFeO_3$	h	−169.48	$Yb_3Fe_5O_{12}$	j	−687.74
Lu_2O_3	C			$LuFeO_3$	h	−169.84	$Lu_3Fe_5O_{12}$	j	−686.14 −686.94
Y_2O_3	C	e	−158.37	$YFeO_3$	i	−168.34	$Y_3Fe_5O_{12}$	j	−684.08

MADELUNG ENERGIES OF $LnFe_2O_4$, $Ln_2Fe_3O_7$, FeO, Fe_3O_4, AND Fe_2O_3 (eV)

Compound	Ref.	U/mole
$YbFe_2O_4$	n	−214.15
YFe_2O_4	Present work	−212.24
FeO	m	−46.72
Fe_3O_4	o	−223.89
α-Fe_2O_3	p	−178.80
$Yb_2Fe_3O_7$	q	−381.57

Note. References for structures: (a) *Mater. Res. Bull.* **14,** 303 (1979); (b) *J. Phys. Chem.* **61,** 753 (1957); (c) *Acta Crystallogr. Sect. B* **35,** 564 (1979); (d) *Z. Anorg. Allg. Chem.* **363,** 1451 (1968); (e) *Acta Crystallogr.* **19,** 307 (1965); (f) Prog. Sci. & Tech. Rare Earths, Vol. 2 (L. Eyring, Ed.), p. 312 (1966); (g) *Mater. Res. Bull.* **6,** 23 (1971); (h) *Acta Crystallogr. Sect. B* **26,** 2008 (1970); (i) *Acta Crystallogr.* **19,** 524 (1965); (j) *Acta Crystallogr.* **19,** 971 (1965); (k) *Izv. Akad. Nauk SSSR Neorg. Mater.* **9,** 871 (1973); (l) *Acta Crystallogr.* **14,** 1051 (1961); (m) ASTM Card 6-0615; (n) *12*(*a*); (o) ASTM Card 19-629; (p) ASTM Card 13-534, (q) *12b*.

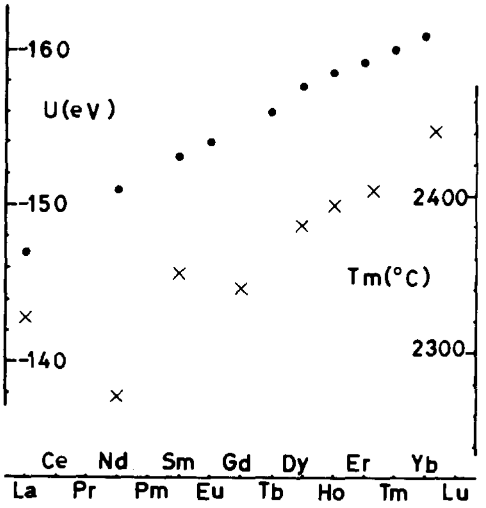

FIG. 1. The Madelung energy ($=U$) and the melting point ($=T_m$) of Ln_2O_3 compounds ●: U; ×: T_m.

tween the enthalpy change and the Madelung energy difference. However, crystallographic transitions of LnFeO$_3$ occur between elevated temperatures and room temperature (*1*, *24*), and the elevated temperature forms are not quenched to room temperature. We considered that the effects of the crystal structural deformations and the thermal change accompanying these phase transitions could not be so great. Using the results of each structural analysis at room temperature, we calculated the Madelung energies of the LnFeO$_3$ and the Ln_2O_3, which are listed in Table III. In the calculations, we used the following hypotheses: (i) a point charge model is used, (ii) repulsive terms of each compound are constant, (iii) the crystal structures at elevated temperatures are frozen in at room temperature, and (iv) the ionic states of the Ln, Fe, and O are Ln^{3+}, Fe^{3+}, and O^{2-} in LnFeO$_3$ and $Ln_3Fe_5O_{12}$, respectively. Using a general computor program developed for any space group, we obtained the results presented in Table III. Since oxide compounds are not typical examples of ionic compounds, we should consider the covalent character for the chemical bonds in the Ln_2O_3 and the LnFeO$_3$ compounds. However, in the case of the Ln_2O_3 compounds, since (i) the dependence of the melting point on the Ln cation (see Fig. 1) (*25*) is consistent with the Madelung energies, and (ii) there are no great differences in the electronegativities (*26a*) of the lanthanide elements (e.g., Gordy and Thomas (*26b*) and Sanderson (*26c*)), we may consider that in a first approximation the bonding character does not significantly change from La_2O_3 (form A) to Lu_2O_3 (form C). In the case of the LnFeO$_3$ compounds, the correspondence between the Madelung energy and the melting points may not be so simple (see Fig. 2) as for Ln_2O_3 (*27*). It may be concluded from the standpoint of melting point measurement that the stability of LnFeO$_3$ crystals with larger Ln cation are much larger than expected from the Made-

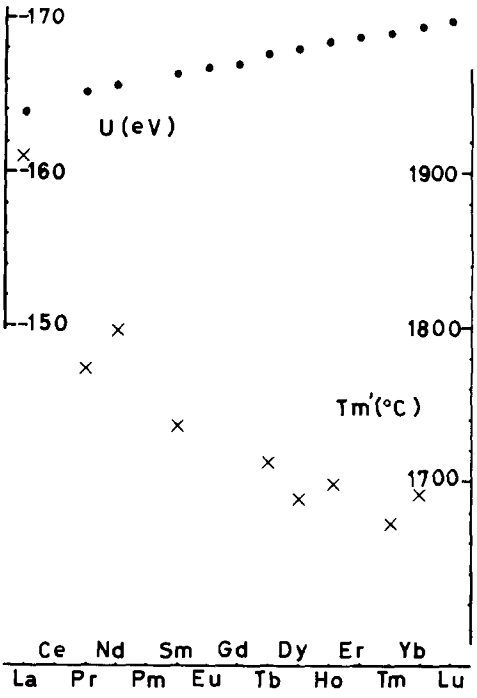

FIG. 2. The Madelung energy ($=U$) and the "crystallographic temperature" ($=T'_m$) of LnFeO$_3$ compounds ●: U; ×: T'_m.

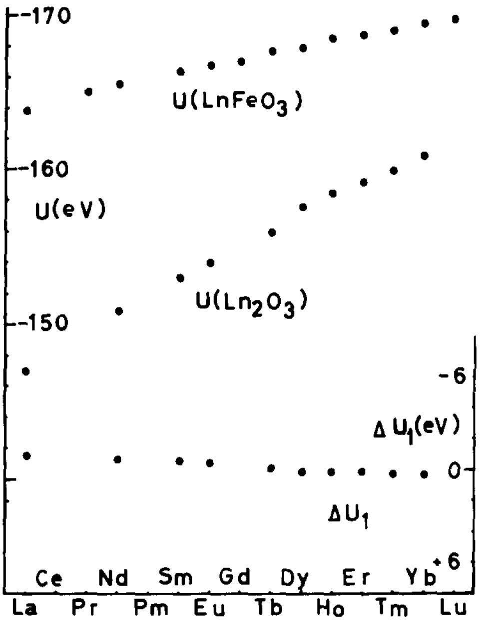

FIG. 3. Madelung energies of $LnFeO_3$, Ln_2O_3, and the Madelung energy difference ($=\Delta U_1$): $U(LnFeO_3) - [U(Ln_2O_3) \times \frac{1}{2} + U(Fe_2O_3) \times \frac{1}{2}]$.

lung energy calculation. However, since it is experimentally difficult to measure each melting point of $LnFeO_3$ compound under an ambient atmosphere, because of the partial reduction of Fe^{3+} to Fe^{2+} in each solid phase (*27*), there seems to be a serious ambiguity concerning the melting point measurements. Nielsen and Blank used the term "crystallographic temperature" instead of melting temperature. Actually, the $LnFeO_3$ phase with a smaller Ln cation is more oxygen deficient under normal pressure (*27, 28*). Marezio *et al.* (*4, 5*) reported that the Fe–O bond distances in the Ln FeO_3 compounds as one proceeds from La FeO_3 to $LuFeO_3$ actually do not alter further, and that the octahedra formed by the Fe–O linking to the other ones tilted further as the constituent Ln cation radius decreases from La to Lu, in order to adjust to a smaller volume of A-site position. In other words, from the viewpoint of crystallographic studies, we can say that the Fe–O bonding character does not change from La to Lu and that the interaction between Ln^{3+} and the hypothetical charged octahedra occurs mainly through a coulombic interaction. Therefore, we concluded from Tables I and II and from Fig. 3 that the dependence of $\Delta G°$ (or $\Delta H°$) upon the constituent Ln cation are mainly attributable to a Madelung energy difference.

(*B*) *Stability of $Ln_3Fe_2Fe_3O_{12}$ (Ln: Sm–Lu and Y)*

The Gibbs free energy changes accompanying the following chemical reaction

$$3LnFeO_3 + \tfrac{2}{3}Fe_3O_4 + \tfrac{1}{6}O_2 = Ln_3Fe_2Fe_3O_{12}$$

is listed in Table IV. Since the reaction rate of the above chemical reaction is very slow, the results of the measurement of the equilibrium oxygen partial pressure have larger experimental errors than those of the Ln FeO_3 compounds. The reaction rate of the decomposition of each garnet becomes slower as the Ln ion radius in each compound is smaller. Therefore, we could not adopt the results of $Lu_3Fe_2Fe_3O_{12}$ and Yb_3 $Fe_2Fe_3O_{12}$ at 1000°C. Using the above data and the $\Delta G°$ values of $LnFeO_3$, FeO, Fe_3O_4, and Fe_2O_3 (*29*), we present the $\Delta G°$ values of the chemical reaction (see Table V)

$$5Fe + \tfrac{3}{2}Ln_2O_3 + \tfrac{15}{4}O_2 = Ln_3Fe_2Fe_3O_{12}.$$

From the temperature dependence of this reaction, $\Delta H°$ and $\Delta S°$ are estimated (see Table VI). $\Delta S° = 44 \times (\frac{15}{4}) = 165$ (e.u.) which as expected from Schmalzried and Navrotsky's conclusion is in good agreement with that of the $Gd_3Fe_2Fe_3O_{12}$.

Piekarczyk *et al.* (*20*) measured the Gibbs free energy change of $Y_3Fe_2Fe_3O_{12}$ by means of a solid state galvanic cell method and reported $\Delta G° = -2078.2 + 0.580T \pm 2.3$ (kJ/mole) in the temperature range of $1173 \leqq T \leqq 1523$ (K). From this result, $\Delta G° = -291.0 \pm 0.6$ (kcal/mole) at 1200°C. As for the $LnFeO_3$ compounds, the Madelung energies of the $Ln_3Fe_2Fe_3O_{12}$

TABLE IV

GIBBS FREE ENERGY CHANGE OF THE CHEMICAL REACTION $3LnFeO_3 + \frac{2}{3}Fe_3O_4 + \frac{1}{6}O_2 = Ln_3Fe_5O_{12}$ ($\Delta G°$(kcal/mole) ± 0.60)

$Ln_3Fe_5O_{12}$	1000°C(a)	1100°C(a)	1150°C(b)	1200°C	1250°C
$Sm_3Fe_5O_{12}$	−8.19	−6.02		−3.20(c)	
$Eu_3Fe_5O_{12}$	−8.87	−6.27		−4.86(d)	
$Gd_3Fe_5O_{12}$	−9.20	−6.75		−5.75(a)	
$Tb_3Fe_5O_{12}$	−9.58	−7.87		−6.55(a)	
$Dy_3Fe_5O_{12}$	−9.55	−7.79		−6.01(a)	
$Ho_3Fe_5O_{12}$	−9.31	−7.44	−6.33	−6.19(b)	−5.08(b)
$Er_3Fe_5O_{12}$	−9.12	−6.94			
$Tm_3Fe_5O_{12}$	−8.40	−6.38	−5.52	−5.52(b)	−4.41(b)
$Yb_3Fe_5O_{12}$		−5.75			
$Lu_3Fe_5O_{12}$		−5.53		−3.36(b)	
$Y_3Fe_5O_{12}$				−6.50(e)	

Note. Refs. (a) *17a*, (b) *17b*, (c) *10a*, (d) *10e*, (e) *10c*.

were calculated (see Table III). The dependence of the Madelung energy difference on the *Ln* ion is also shown in Fig. 4. From these results, one can say that the dependence of $\Delta G°$ or $\Delta H°$ upon the *Ln* cation and that of ΔU_2 are very similar. The free energy change in the chemical reaction

$$3LnFeO_3 + \tfrac{2}{3}Fe_3O_4 + \tfrac{1}{6}O_2 = Ln_3Fe_2Fe_3O_{12}$$

or

$$3LnFeO_3 + Fe_2O_3 = Ln_3Fe_2Fe_3O_{12}$$

indicates a maximum change in $-\Delta G°$ near Ln = Tb. The Madelung energy difference corresponding to the above chemical reaction is shown in Fig. 5. $-\Delta U_2'$ shows a maximum value near Ln = Tb or Gd.

In the garnet structure, there are dodecahedral (*Ln*–O), octahedral (Fe–O), and tetrahedral (Fe–O) polyhedra which share a common edge. Esipinosa (*30*) plotted lattice constant of $Ln_3Fe_2Fe_3O_{12}$ vs atomic number of the rare earth element and found a double festoon curve which is caused by a

TABLE V

GIBBS FREE ENERGY CHANGE OF THE CHEMICAL REACTION $5Fe + \frac{3}{2}Ln_2O_3 + \frac{15}{4}O_2 = Ln_3Fe_3O_{12}$ ($\Delta G°$(kcal/mole) ± 0.60)

$Ln_3Fe_5O_{12}$	1000°C(a)	1100°C(a)	1150°C(b)	1200°C	1250°C
$Sm_3Fe_5O_{12}$	−332.5	−315.6		−298.5(c)	
$Eu_3Fe_5O_{12}$	−331.7	−314.0		−297.8(d)	
$Gd_3Fe_5O_{12}$	−330.9	−313.6		−298.8(a)	
$Tb_3Fe_5O_{12}$	−328.6	−311.6		−295.5(a)	
$Dy_3Fe_5O_{12}$	−326.7	−309.1		−293.2(a)	
$Ho_3Fe_5O_{12}$	−325.9	−306.9	−295.7	−288.5(b)	−284.4(b)
$Er_3Fe_5O_{12}$	−323.6	−304.3		−286.2(c)	
$Tm_3Fe_5O_{12}$	−322.9	−301.0	−289.2	−284.5(b)	−277.5(b)
$Yb_3Fe_5O_{12}$		−298.4		−283.4(e)	
$Lu_3Fe_5O_{12}$		−295.9		−279.1(c)	
$Y_3Fe_5O_{12}$				−288.9(*f*)	

Note. Refs. (a) *17a*, (b) *17b*, (c) *10a*, (d) *10e*, (e) *10d*, (f) *10c*.

TABLE VI

ENTHALPY CHANGE AND ENTROPY CHANGE: $5Fe + \frac{3}{2}Ln_2O_3 + \frac{15}{4}O_2 = Ln_3Fe_5O_{12}$

$Ln_3Fe_5O_{12}$	ΔH°(kcal/mole)	ΔS°(e.u.)
$Sm_3Fe_5O_{12}$	−549 ± 10	−170 ± 10
$Eu_3Fe_5O_{12}$	−549 ± 10	−171 ± 10
$Gd_3Fe_5O_{12}$	−548 ± 10	−171 ± 10
$Tb_3Fe_5O_{12}$	−542 ± 10	−168 ± 10
$Dy_3Fe_5O_{12}$	−536 ± 10	−165 ± 10
$Ho_3Fe_5O_{12}$	−524 ± 10	−158 ± 10
$Er_3Fe_5O_{12}$	−512 ± 10	−151 ± 10
$Tm_3Fe_5O_{12}$	−506 ± 10	−150 ± 10
$Yb_3Fe_5O_{12}$	−510 ± 10	−153 ± 10
$Lu_3Fe_5O_{12}$	−494 ± 10	−145 ± 10
$Y_3Fe_5O_{12}$		

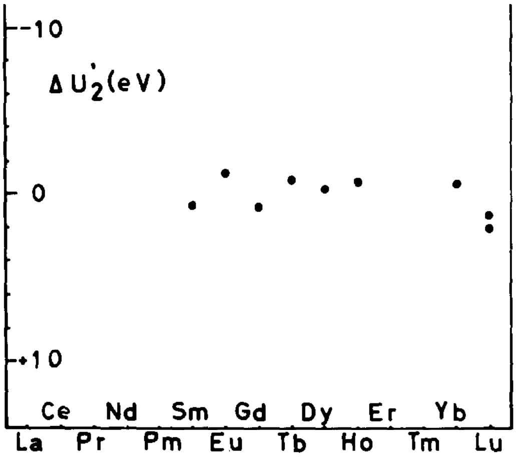

FIG. 5. Madelung energy difference ($=\Delta U_2'$): $U(Ln_3Fe_5O_{12}) - [U(LnFeO_3) \times 3 + U(Fe_2O_3)]$.

small crystal field effect on the nonspherical Ln ion. The interatomic distances are mainly dependent upon the ionic radius of the Ln ion. Thus we can easily presume that there should be an optimum Ln ion in the dodecahedron which is able to share the common edges with the octahedra and the tetrahedra. La, Pr, and Nd are too large to form the dodecahedron together with the octahedron and the tetrahedron formed by the Fe^{3+}–O bonds. The elements indium and scandium are too small to exist in the dodecahedron under normal pressure. We may conclude that thermochemical data, crystallographic data, and a simple ionic charge model point to a consistent result as to the dependence of the stability of each $Ln_3Fe_2Fe_3O_{12}$ compound on the Ln cation. The $Ln_3Fe_2Fe_3O_{12}$, $LnFe_2O_4$, and $Ln_2Fe_3O_7$ have incongruent melting points (*28*), therefore we did not compare the Madelung energies with each melting point.

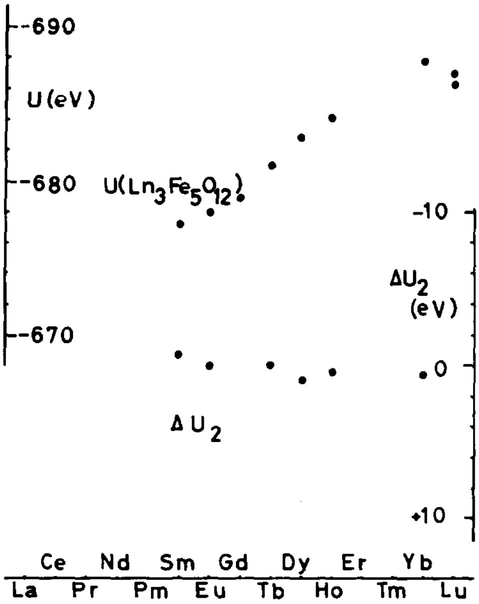

FIG. 4. Madelung energy of $Ln_3Fe_5O_{12}$ and the Madelung energy difference ($=\Delta U_2$): $U(Ln_3Fe_5O_{12}) - [U(Ln_2O_3) \times \frac{3}{2} + U(Fe_2O_3) \times \frac{5}{2}]$.

(C) Stability of $LnFe_2O_4$ (Ln: Ho–Lu and Y) and $Ln_2Fe_3O_7$ (Ln: Yb and Lu)

The free energy changes accompany the following chemical reaction are listed in Table VII(a):

$$2Fe + \tfrac{1}{2}Ln_2O_3 + \tfrac{5}{4}O_2 = LnFe_2O_4.$$

We did not estimate the enthalpy change and the entropy change of the above chemical reaction, because of the very narrow range of temperature. Since the $\Delta H°$ values

TABLE VII(a)

GIBBS FREE ENERGY CHANGE OF THE CHEMICAL REACTION $2Fe + \frac{1}{2}Ln_2O_3 + \frac{5}{4}O_2 = LnFe_2O_4$ ($\Delta G°$(kcal/mole) ± 0.50)

$LnFe_2O_4$	1000°C	1100°C	1150°C	1200°C	1250°C
$HoFe_2O_4$				−100.9(a)	−99.3(a)
$ErFe_2O_4$		−105.2(b)		−100.8(c)	
$TmFe_2O_4$	−111.3(b)	−104.9(b)	−101.8(a)	−100.6(a)	−99.04(b)
$YbFe_2O_4$		−105.1(b)		−100.4(d)	
$LuFe_2O_4$		−104.5(b)	−101.4(a)	−100.3(a)	−98.55(a)
$YFe_2O_{3.905}$				−96.8(d)	

Note. Refs. (a) *17a*, (b) *17b*, (c) *10g*, (d) *10c*.

are about three times larger than the $T\Delta S°$ values, and $\Delta S°$ is actually constant, the dependencies of $\Delta G°$ and $\Delta H°$ on the constituent *Ln* cation element exhibit similar trends. Therefore, we can compare $\Delta G°$ instead of $\Delta H°$ with the Madelung energy difference. As the crystal structure analysis of $YbFe_2O_4$ had been performed by Kato *et al.* (*12a*), we refined the crystal structure of YFe_2O_4 and obtained the dependence of the Madelung energy of the $LnFe_2O_4$ compounds on the *Ln* cation. The experimental conditions and the results obtained for the refinement are shown in Table VIII.

The free energy changes in the chemical reaction $LnFeO_3 + FeO = LnFe_2O_4$ (*Ln*: Ho, Er, Tm, Yb, Lu, and Y) are estimated (see Table VII(b). $LnFe_2O_4$ becomes more stable as the size of the *Ln* decreases and the temperature increases. As reported earlier (*17b*), each $LnFe_2O_4$ phase decomposes to $LnFeO_3$ and FeO at a certain temperature. The lower limits of the stability range in temperature are $HoFe_2O_4$: 1175°C, $ErFe_2O_4$: 1050°C, $TmFe_2O_4$: 950°C, and $LuFe_2O_4$: 900°C (*17a*). Although the $\Delta H°$ in

TABLE VII(b)

$LnFeO_3 + FeO = LnFe_2O_4$ ($\Delta G°$(kcal/mole) ± 0.50)

$LnFe_2O_4$	1000°C	1100°C	1150°C	1200°C	1250°C
$HoFe_2O_4$				−0.2(a)	−0.4(a)
$ErFe_2O_4$		−0.2(b)		−0.7(c)	
$TmFe_2O_4$	−0.3(b)	−1.3(b)	−1.4(a)	−1.7(a)	−2.1(b)
$YbFe_2O_4$		−2.0(b)		−2.0(d)	
$LuFe_2O_4$		−2.3(b)	−2.6(a)	−2.7(a)	−3.0(a)

Note. Refs. (a) *17a*, (b) *17b*, (c) *10g*, (d) *10c*.

TABLE VIII

STRUCTURAL REFINEMENT OF YFe_2O_4

Experimental conditions	
Crystal size	0.27 × 0.20 × 0.05 mm
Wave length	Mo$K\alpha$
Monochrometer	Graphite ($2\theta_M$ = 12.17°)
Intensity measurement	Four-circle goniometer system
Counting system	Scintillation counter
Measurement range	$h \geqq 0$, $k \geqq 0$, $110° \geqq 2\theta \geqq 0$
Number of observed reflections	990
Number of nonzero reflections	758
Number of independent nonzero reflections	428
Correction	Lorentz polarization, absorption (for μ = 228 cm^{-1}), extinction, and dispersion effects

Experimental result	
Possible space group	$R\bar{3}m$
Lattice constants	a = 3.516(1) Å, c = 24.79(2) Å

Atom position

Atom	Position	x	y	z	β_{11}	β_{33}
Y	3a	0	0	0	0.0093(7)	0.00218(4)
Fe	6c	0	0	0.21440(6)	0.043(1)	0.00030(1)
O(1)	6c	0	0	0.2924(2)	0.040(9)	0.0031(8)
O(2)	6c	0	0	0.1282(4)	0.089(7)	0.00097(14)

R = 0.116, weighted R = 0.055

the chemical reaction $LnFeO_3$ + FeO = $LnFe_2O_4$ is erroneous, as mentioned above, we could estimate that ΔH° is positive (endothermic). The Madelung energy differences are $\Delta U_3 = U(LnFe_2O_4) - [U(LnFeO_3) + U(FeO)] = 2.07$ for Ln = Yb and 2.48 for Ln = Y. We can state that the dependencies of the ΔG° and ΔU_3 on the Ln cation are similar. In the $LnFe_2O_4$ phase, Fe^{3+} and Fe^{2+} occupy one trigonal bipyramidal site and the Ln ion occupies an octahedral site. Since it is more difficult for Ln which is larger than Dy to form the octahedron, coexisting with the trigonal bipyramid formed by the $Fe^{2.5+}$–O bonds in the $LnFe_2O_4$ phase, only the $LnFe_2O_4$ (*Ln:* Ho, Er, Tm, Yb, Lu, and Y) are stable in each phase diagram of the Ln_2O_3–FeO–Fe_2O_3 systems above a certain temperature, respectively. Therefore, it is reasonable that the free energy change and the Madelung energy difference have a similar dependence on the constituent Ln cation.

The free energy changes of $Yb_2Fe_3O_7$ and $Lu_2Fe_3O_7$ are shown in Tables IX(a) and (b). As we know only one crystal structural datum of the $Yb_2Fe_3O_7$, we cannot present the dependence of the Madelung energy upon the constituent Ln cation. Only $\Delta U = U(Yb_2Fe_3O_7) - [2 \times U(YbFeO_3) + U(FeO)] = 4.13$ (endothermic) is obtained. As in the case of $LnFe_2O_4$, $Ln_2Fe_3O_7$ is more stable as the Ln element in the phase becomes smaller and the temperature increases (see Table IX(b)). $Tm_2Fe_3O_7$ does not exist at 1200°C as a stable phase; however, it is stable above 1350°C (*17b*). Since there are Fe_4O_5 layers and Fe_2O_3 layers which sandwich the Ln–O octahedron in the $Ln_2Fe_3O_7$ structure, the bond distances of Ln–O in the octahedron have more restricted values than in the $LnFe_2O_4$ structure. Thus, only Yb and Lu form the $Ln_2Fe_3O_7$ structure.

TABLE IX(a)

GIBBS FREE ENERGY CHANGE OF THE CHEMICAL REACTION 3Fe + Ln_2O_3 + $2O_2$ = $Ln_2Fe_3O_7$ (ΔG°(kcal/mole) ± 0.5)

$Ln_2Fe_3O_7$	1100°C	1150°C	1200°C	1250°C
$Yb_2Fe_3O_7$	−166.6(a)		−158.4(b)	
$Lu_2Fe_3O_7$	−166.6(a)	−160.2(c)	−158.2(c)	−155.0(c)

Note. Refs. (a) *17a*, (b) *10d*, (c) *17b*.

TABLE IX(b)

$2LnFeO_3$ + FeO = $Ln_2Fe_3O_7$ (ΔG°(kcal/mole) ± 0.5)

$Ln_2Fe_3O_7$	1100°C	1150°C	1200°C	1250°C
$Yb_2Fe_3O_7$	−2.1(a)		−2.2(b)	
$Lu_2Fe_3O_7$	−2.8(a)	−3.0(c)	−3.1(c)	−3.4(c)

Note. Refs. (a) *17a*, (b) *10d*, (c) *17b*.

There is only one crystallographic site of the Ln ion in $LnFeO_3$, in $Ln_3Fe_2Fe_3O_{12}$, in $LnFe_2O_4$, and in $Ln_2Fe_3O_7$; therefore, it is easy to observe the effect of the Ln ion size on the Fe–O bonds in each phase. For the $LnFeO_3$ compounds reported in (*1, 4, 5*), the Fe–O distances varied between 2.006 and 2.14 Å. For the $Ln_3Fe_2Fe_3O_{12}$ compounds (*7–9*) the distances ranged from 2.00 to 2.039 Å, and 1.861 to 1.89 Å for the octahedral and tetrahedral sites, respectively; in $YbFe_2O_4$, YFe_2O_4, and $Yb_2Fe_3O_7$ the $Fe^{2.5+}$–O distances are 2.026, 2.041, and 1.998 Å, respectively (*12a, 12b*). In $Yb_2Fe_3O_7$ the Fe^{3+}–O bond length is 1.974 Å (*12b*). Thus we can safely conclude that there is no significant bonding character change in each of the Fe–O and the Ln–O bonds in the $LnFeO_3$ compounds, the $Ln_3Fe_2Fe_3O_{12}$ compounds, and the $(LnFeO_3)_nFeO$ compounds. The dependencies of the free energy changes of each phase on the Ln cation should be mainly attributed to the Madelung energy difference in each chemical reaction.

Conclusions

(1) We summarized the thermochemical data of the stable phases, $LnFeO_3$, Ln_3Fe_2

Fe_3O_{12}, $LnFe_2O_4$, and $Ln_2Fe_3O_7$ in the Ln_2O_3–FeO–Fe_2O_3 systems in the temperature range 1000–1400°C.

(2) To understand the thermochemical data of the phases in the above systems, we calculated the Madelung energies of the stable phases, based upon a simple point charge ionic model. The $LnFeO_3$ compounds are less stable; $Ln_3Fe_2Fe_3O_{12}$ is most stable near Ln = Tb, and (Ln $FeO_3)_nFeO$ ($n = 1$ and 2) are more stable as the Ln cation in each phase becomes smaller.

(3) As the Fe–O bond distances in Ln FeO_3 and in $Ln_3Fe_2Fe_3O_{12}$ are almost independent of the Ln cation, the changes in each crystal structure are absorbed by the environment around the Ln cation, and the electronegativity does not change much from La to Lu. We concluded that we could estimate the dependence of the free energy changes on the Ln cation through calculations of the Madelung energy.

(4) To estimate the phase relations in a series of phase diagrams in which isostructural phases exist, it is qualitatively useful to calculate the Madelung energy of each phase in advance. The absolute value of the Madelung energy difference of each chemical reaction is almost meaningless for understanding the chemical bonds in the oxide compounds. However, we may note a systematic relative change in energy corresponding to a change of the interatomic distances in a series of isostructural compounds, through calculations of the Madelung energies of each compound, if each component element has a similar electronegativity.

Acknowledgments

One of the authors (N.K.) expresses his sincere thanks to Dr. T. Chiba, Dr. T. Akahane, and Dr. T. Kikuchi of the National Institute for Research in Inorganic Materials for helpful discussions.

References

1. S. Geller and E. W. Wood, *Acta Crystallogr.* **9,** 563 (1956).
2. S. Geller, *J. Chem. Phys.* **24,** 1236 (1956).
3. P. Coppens and M. Eibschütz, *Acta crystallogr.* **19,** 524 (1965).
4. M. Marezio, J. P. Remeika, and P. D. Dernier, *Acta Crystallogr. Sect. B* **26,** 2008 (1970).
5. M. Marezio and P. Dernier, *Mater. Res. Bull.* **6,** 23 (1971).
6. S. Geller and M. A. Gilleo, *J. Phys. Chem. Solids* **3,** 30 (1957).
7. F. Euler and J. A. Bruce, *Acta Crystallogr.* **19,** 871 (1965).
8. J. Weidenborner, *Acta Crystallogr.* **14,** 1051 (1961).
9. E. L. Dukhovskya, Yu G. Saksonov, and A. G. Titov, *Izv. Akad. Nauk SSSR Neorg. Mater.* **9,** 809 (1973).
10. (a) T. Katsura, K. Kitayama, T. Sugihara and N. Kimizuka, *Bull. Chem. Soc. Japan* **48,** 1809 (1975); (b) N. Kimizuka and T. Katsura *Bull. Chem. Soc. Japan* **47,** 1801 (1974); (c) N. Kimizuka and T. Katsura, *J. Solid State Chem.* **13,** 176 (1975); (d) N. Kimizuka and T. Katsura, *J. Solid State Chem.* **15,** 151 (1975); (e) T. Sugihara, N. Kimizuka, and T. Katsura, *Bull. Chem. Soc. Japan* **48,** 1806 (1975); (f) T. Katsura, T. Sekine, K. Kitayama, T. Sugihara, and N. Kimizuka, *J. Solid State Chem.* **23,** 43 (1978); (g) K. Kitayama and T. Katsura, *Bull. Chem. Soc. Japan* **49,** 998 (1976).
11. A. Navrotsky, *in* "Structure and Bonding in Crystal II" (M. O'Keeffe and A. Navrotsky, Eds.), Chap. 17, pp. 71–92, Academic Press, New York (1981).
12. (a) K. Kato, I. Kawada, N. Kimizuka, and T. Katsura, *Z. Kristallogr.* **141,** 314 (1975); (b) K. Kato, I. Kawada, N. Kimizuka, I. Shindo, and T. Katsura, *Z. Kristallogr.* **143,** 278 (1976); (c) Y. Matsui, K. Kato, N. Kimizuka, and S. Horiuchi, *Acta Crystallogr. Sect. B* **35,** 561 (1979); (d) N. Kimizuka, K. Kato, I. Kawada, I. Shindo, and T. Katsura, *Acta Crystallogr. Sect. B* **32,** 1721 (1976); (e) B. Malaman, O. Evrard, N. Tannieres, and J. Aubry, *Acta Crystallogr. Sect. B* **31,** 1310 (1975); (f) B. Malaman, O. Evrard, and J. Aubry, *Acta Crystallogr. Sect. B* **32,** 749 (1980).
13. R. Geradin, A. Alebouyeh, F. Jeannot, A. Courtois, B. Malaman, and O. Evrard, *Mater. Res. Bull.* **15,** 647 (1980).
14. (a) M. Inazumi, Y. Nakagawa, M. Tanaka, N. Kimizuka, and K. Siratori, *J. Phys. Soc. Japan* **50,** 438 (1981); (b) J. Akimitsu, Y. Inada, K.

SIRATORI, I. SHINDO, AND N. KIMIZUKA, *Solid State Commun.* **32,** 1065 (1979); (c) Y. NAKAGAWA, M. KISHI, H. HIROYOSHI, N. KIMIZUKA, AND K. SIRATORI, *Ferrites,* 115 (1980); (d) M. TANAKA, J. AKIMITSU, I. SHINDO, N. KIMIZUKA, AND K. SIRATORI, *Ferrites,* 119 (1980); (e) M. TANAKA, M. KATO, N. KIMIZUKA, AND K. SIRATORI, *J. Phys. Soc. Japan* **47,** 1737 (1979); (f) M. KISHI, S. MIURA, Y. NAKAGAWA, N. KIMIZUKA, I. SHINDO, AND K. SIRATORI, *J. Phys. Soc. Japan* **51,** 2801 (1982).

15. (a) N. KIMIZUKA AND E. TAKAYAMA, *J. Solid State Chem.* **40,** 109 (1981); (b) N. KIMIZUKA AND E. TAKAYAMA, *J. Solid State Chem.* **41,** 166 (1982); (c) N. KIMIZUKA AND E. TAKAYAMA, *J. Solid State Chem.* **42,** 22 (1982); (d) N. KIMIZUKA AND E. TAKAYAMA, *J. Solid State Chem.* **43,** 278 (1982).
16. T. ARAKAWA, S. TSUCHI-YA, AND J. SHIOKAWA, *Mater. Res. Bull.* **16,** 97 (1981).
17. (a) T. SUGIHARA, Thesis of D.Sc. (in Japanese) 1979, Dept. of Chemistry, Faculty of Science, Tokyo Institute of Technology, Meguro-ku, Tokyo, Japan, 152; (b) T. SEKINE, Thesis of M.S. (in Japanese) 1978, Dept. of Chemistry, Faculty of Science, Tokyo Institute of Technology, Meguro-ku, Tokyo, Japan 152.
18. J. MIZUSAKI, T. SASAMOTO, W. R. CANNON, AND H. K. BOWEN, *J. Amer. Ceram. Soc.* **65,** 363 (1982).
19. T. NAKAMURA, G. PETZOW, AND L. J. GANCKLER, *Mater. Res. Bull.* **14,** 649 (1979).
20. W. PIEKARCZYK, W. WEPPENER, AND A. RABENAU, *Mater. Res. Bull.* **13,** 1077 (1978).
21. YU D. TRETYAVOV, A. R. KAUL, AND V. K. PORTONY, *High Temp. Sci.* **9,** 61 (1977).
22. H. SCHMALTZRIED AND A. NAVROTZKY, "Festkörperthermodynamik," p. 119, Verlag Chemie, Weinheim (1975).
23. T. NAKAMURA, *J. Solid State Chem.* **38,** 229 (1981).
24. S. GELLER AND R. M. RACCAH, *Phys. Rev. Sect. B* **2,** 1167 (1970).
25. O. KUBASCHEWSKI AND C. B. ALCOCK, "Metallurgical Thermochemistry," 5th ed., Pergamon, New York (1979).
26. (a) L. PAULING, "The Nature of the Chemical Bond" 3rd. ed., Chap. 3, Cornell Univ. Press, Ithaca, N.Y. (1960); (b) W. GORDY AND W. O. THOMAS, *J. Chem. Phys.* **24,** 439 (1956); (c) S. T. SANDERSON, "Inorganic Chemistry" (in Japanese), Chap. 12, p. 260, Hirokawa Shoten, Tokyo (1967).
27. J. W. NIELSEN AND S. L. BLANK, *J. Cryst. Growth* **13/14,** 702 (1972).
28. I. SHINDO, N. KIMIZUKA, AND S. KIMURA, *Mater. Res. Bull.* **11,** 637 (1976).
29. "JANAF Thermochemical Table," 2nd. ed., NSRDS-NBS (1971).
30. G. P. ESPINOSA, *J. Chem. Phys.* **37,** 2344 (1962).